Т. 9. №6. 2023
https://doi.org/10.33619/2414-2948/91

UDC 621.548.4 https://doi.org/10.33619/2414-2948/91/39

RESEARCH ON MODELING AND SIMULATION OF DOUBLY FED INDUCTION WIND TURBINE BASED ON MATLAB/SIMULINK

©Zheng Shouqing, *ORCID: 0009-0000-2442-616X, Jiangsu University of Science and Technology, Zhenjiang, China, qqqd_zsq@163.com*
©Bai Yike, *Jiangsu University of Science and Technology, Zhenjiang, China, 935148103@qq.com*
©Hou Ruida, *Jiangsu University of Science and Technology, Zhenjiang, China, 553774347@qq.com*
©Wang Bao Liang, *ORCID: 0009-0009-5218-3877, Jiangsu University of Science and Technology, Zhenjiang, China, 1067358144@qq.com*

ИССЛЕДОВАНИЯ ПО МОДЕЛИРОВАНИЮ ВЕТРОУСТАНОВКИ С ДВОЙНЫМ ПИТАНИЕМ НА ОСНОВЕ MATLAB/SIMULINK

©Чжэн Шоуцин, *ORCID: 0009-0000-2442-616X, Цзянсуский университет науки и технологии, г. Чжэньцзян, Китай, qqqd_zsq@163.com*
©Бай Икэ, *Цзянсуский университет науки и технологии, г. Чжэньцзян, Китай, 935148103@qq.com*
©Хоу Жуйда, *Цзянсуский университет науки и технологии, г. Чжэньцзян, Китай, 553774347@qq.com*
©Ван Бао Лян, *ORCID: 0009-0009-5218-3877, Цзянсуский университет науки и технологии, г. Чжэньцзян, Китай, 1067358144@qq.com*

Abstract. This paper first introduces the structure of doubly-fed wind power generation system and the working principle of doubly-fed induction generator in detail, and establishes the corresponding mathematical model of doubly-fed wind power generation unit. The control part of wind power generation system based on doubly-fed induction generator includes rotor side control and stator side control. The rotor side control adopts the vector control strategy based on stator flux orientation of the double-fed induction generator connected to the grid, and the working principle is analyzed in detail, and the main part of the simulation modeling is given. Stator side control adopts vector control strategy of grid-connected inverter control, and its working principle is analyzed in detail, and the main part of simulation modeling is also given. In order to verify the correctness and feasibility of the system, the simulation experiment platform of doubly fed wind turbine under this control strategy is built by using Matlab/Simulink simulation platform, and its simulation analysis is carried out in detail.

Аннотация. Подробно представлена структура ветровой электростанции с двойным питанием и принцип работы асинхронного генератора с двойным питанием, а также установлена соответствующая математическая модель ветровой электростанции с двойным питанием. Управляющая часть ветроэнергетической системы на базе асинхронного генератора двойного питания включает управление со стороны ротора и управление со стороны статора. Управление со стороны ротора использует стратегию векторного управления, основанную на ориентации потока статора асинхронного генератора с двойным питанием, подключенного к сети, и подробно анализируется принцип работы, и дается основная часть имитационного моделирования. Управление со стороны статора использует стратегию векторного управления инвертором, подключенным к сети, и его принцип работы подробно анализируется, а также

Т. 9. №6. 2023
https://doi.org/10.33619/2414-2948/91

дается основная часть имитационного моделирования. Чтобы проверить правильность и осуществимость системы, платформа эксперимента по моделированию ветровой турбины с двойным питанием в соответствии с этой стратегией управления построена с использованием платформы моделирования Matlab / Simulink, и ее анализ моделирования выполнен в деталях.

Keywords: Doubly-fed wind turbine, Vector control, Simulink simulation, Decoupling control.

Ключевые слова: ветряная турбина с двойным питанием, векторное управление, моделирование Simulink, управление развязкой.

The rapid development of society leads to the rapid depletion of energy resources. All countries are at a critical moment of environmental protection. The top priority is to develop new energy resources. New energy usually refers to renewable energy, which mainly includes: solar energy, tidal energy, wind energy, geothermal energy and biological energy. The essence of wind energy is the kinetic energy generated by a large amount of air flowing on the earth's surface. It is one of the environment-friendly and pollution-free energy sources. The advantage of wind power is inexhaustible, inexhaustible, and the use of wind power generation infrastructure cycle is short, flexible installation scale. Wind energy has very low requirements for application. It is very suitable to use wind power according to local conditions in coastal islands, grassland pastoral areas, mountainous areas and plateau areas where water shortage, fuel shortage and traffic underdeveloped, and has broad development prospects [1].

Doubly-fed wind turbine is one of the most widely used turbines. Because the excitation converter has the characteristic of only transmitting the differential power, the capacity required by the converter is very small, which reduces the cost of the converter. It is especially suitable for large-scale wind farms. By adjusting the amplitude, phase and frequency of the rotor excitation current by power electronic device, the generator can operate at VSCF in a wide range of synchronous speed. The speed of the wind turbine is adjusted according to the change of wind speed in real time, so that the unit can keep running under the optimal speed and realize the tracking control of the maximum wind energy [2].

Doubly fed wind turbine is based on doubly fed induction generator (DFIG), this paper first analyzes the structure characteristics, working mode and operating principle of doubly-fed induction generator. Based on the mathematical model of the generator, the corresponding simulation model was built with Simulink in MATLAB. According to the principle of vector control, the grid side converter and rotor side converter are designed. Finally, the simulation model of doubly fed wind turbine is established. Under the changing wind speed, the frequency, amplitude and phase of rotor excitation current are adjusted by converter to maintain the electric energy output of constant frequency, and then the independent regulation of reactive power and active power is realized by vector control principle [3, 4].

Material and research methods

Mathematical model of doubly fed induction generator in three-phase static coordinate system. In this section, the mathematical model of doubly fed induction motor is analyzed in detail. The stator side follows the generator convention, and the stator current is positive with outflow; The rotor side follows the motor practice, and the outflow of rotor current is negative. In order to establish the mathematical model, the following assumptions are generally made [5]:

1. The included angle of symmetrical three-phase windings of stator and rotor in space is

Т. 9. №6. 2023
https://doi.org/10.33619/2414-2948/91

120°, and the magnetomotive force is distributed on the circumference of air gap in the law of sinusoidal curve. Under the influence of fundamental magnetic field, only air gap harmonic magnetic field can be considered in differential leakage reactance, and the influence of tooth harmonic can not be calculated because the surface of stator and rotor is smooth.

2. The effects of iron loss and nonlinear ferromagnetism can be ignored.

3. The temperature rise of stator and rotor windings can be ignored.

4. The parameters of the rotor side of the doubly fed induction motor are converted to the stator side, and the number of turns of the stator after conversion is equal to that of the rotor.

1. Voltage equation. Stator winding voltage equation:

$$u_1 = -R_1 i_1 + p\psi_1 \tag{1}$$

Rotor winding voltage equation:

$$u_2 = R_2 i_2 + p\psi_2 \tag{2}$$

Where, u_1 and u_2 are instantaneous values of stator and rotor phase voltage respectively. i_1 and i_2 are instantaneous values of stator and rotor phase currents respectively. Ψ_1 and Ψ_2 are stator and rotor winding flux chains respectively. R_1 and R_2 are the resistances of stator winding and rotor winding respectively. p is the differential operator, instead of the differential sign d/dt.

Rewrite the above equation into the matrix form in the three-phase stationary coordinate system:

$$\begin{bmatrix} u_{a1} \\ u_{b1} \\ u_{c1} \\ u_{a2} \\ u_{b2} \\ u_{c2} \end{bmatrix} = \begin{bmatrix} R_1 & 0 & 0 & 0 & 0 & 0 \\ 0 & R_1 & 0 & 0 & 0 & 0 \\ 0 & 0 & R_1 & 0 & 0 & 0 \\ 0 & 0 & 0 & R_2 & 0 & 0 \\ 0 & 0 & 0 & 0 & R_2 & 0 \\ 0 & 0 & 0 & 0 & 0 & R_2 \end{bmatrix} \begin{bmatrix} -i_{a1} \\ -i_{b1} \\ -i_{c1} \\ i_{a2} \\ i_{b2} \\ i_{c2} \end{bmatrix} + p \begin{bmatrix} \psi_{a1} \\ \psi_{b1} \\ \psi_{c1} \\ \psi_{a2} \\ \psi_{b2} \\ \psi_{c2} \end{bmatrix} \tag{3}$$

Where, $u_{a1}, u_{b1}, u_{c1}, i_{a1}, i_{b1}, i_{c1}$ are instantaneous values of stator phase voltage and phase current. $u_{a2}, u_{b2}, u_{c2}, i_{a2}, i_{b2}, i_{c2}$ are instantaneous values of rotor phase voltage and phase current. $\Psi_{a1}, \Psi_{b1}, \Psi_{c1}$ are the flux linkage value of stator winding. $\Psi_{a2}, \Psi_{b2}, \Psi_{c2}$ are the flux linkage value of rotor winding[6].

2. Flux linkage equation. Simplify the above complex equation and express the flux linkage equation in matrix form as:

$$\begin{bmatrix} \psi_1 \\ \psi_2 \end{bmatrix} = \begin{bmatrix} L_{11} & L_{12} \\ L_{21} & L_{22} \end{bmatrix} \begin{bmatrix} i_1 \\ i_2 \end{bmatrix} \tag{4}$$

Where,

$$\psi_1 = [\psi_{a1} \psi_{b1} \psi_{c1}]^T$$
$$\psi_2 = [\psi_{a2} \psi_{b2} \psi_{c2}]^T$$
$$i_1 = -[i_{a1} i_{b1} i_{c1}]^T$$
$$i_2 = -[i_{a2} i_{b2} i_{c2}]^T$$

3. Torque equation

Т. 9. №6. 2023
https://doi.org/10.33619/2414-2948/91

$$T_e = \frac{1}{2} n_p \left[i_2^{\ T} \frac{dL_{21}}{d\theta} i_1 + i_1^{\ T} \frac{dL_{12}}{d\theta} i_2 \right] \quad (5)$$

Where,$T_e$is electromagnetic torque. $n_p$is the number of poles of doubly fed machine.

4. Equation of motion

$$T_L - T_e = \frac{J}{n_p} \frac{d\omega_r}{dt} \quad (6)$$

Where,T_L is the mechanical torque input by the wind turbine. ω_r is the rotor rotation angular speed of the generator. J is the moment of inertia of the unit [7].

Mathematical model of doubly fed induction generator in synchronous rotating coordinate system. As mentioned above, the mutual inductance between stator and rotor changes with the change of relative position between stator and rotor when the motor rotor rotates, which makes the doubly fed induction generator have the characteristics of variability and strong coupling. Due to the changes of stator and rotor in the working process of generator, the design and control of motor are more complex. Therefore, based on the coordinate transformation technology, the mathematical model in the two-phase synchronous rotating coordinate system can be obtained by converting the equation in the three-phase static coordinate system to the d-q coordinate system [8]:

1. Voltage equation. Stator winding voltage equation:

$$\begin{cases} u_{d1} = -R_1 i_{d1} - p\psi_{d1} + \omega_1 \psi_{q1} \\ u_{q1} = -R_1 i_{q1} - p\psi_{q1} + \omega_1 \psi_{d1} \end{cases} \quad (7)$$

Rotor winding voltage equation:

$$\begin{cases} u_{d2} = R_2 i_{d2} + p\psi_{d2} - \omega_s \psi_{q2} \\ u_{q2} = R_2 i_{q2} + p\psi_{q2} + \omega_s \psi_{d2} \end{cases} \quad (8)$$

Where, u_{d1} , u_{q1} , u_{d2} and u_{q2} are d-q axis components of stator and rotor voltage respectively. i_{d1} , i_{q1} , i_{d2} and i_{q2} are d-q axis components of stator and rotor current respectively. $\Psi_{d1}, \Psi_{q1}, \Psi_{d2}$ and Ψ_{q2} are d-q axis components of stator and rotor flux linkage respectively[9].

2. Flux linkage equation. Stator flux equation:

$$\begin{cases} \psi_{d1} = L_1 i_{d1} - L_m i_{d2} \\ \psi_{q1} = L_1 i_{q1} - L_m i_{q2} \end{cases} \quad (9)$$

Rotor flux equation:

$$\begin{cases} \psi_{d2} = L_2 i_{d2} - L_m i_{d1} \\ \psi_{q2} = L_2 i_{q2} - L_m i_{q1} \end{cases} \quad (10)$$

Where,$L_1$is the self inductance of equivalent two-phase stator winding.L_2 is the self inductance of equivalent two-phase rotor winding.L_m is the equivalent mutual inductance between coaxial stator and rotor windings [10].

3. Torque equation:

$$T_e = n_p \left(\psi_{q1} i_{d1} - \psi_{d1} i_{q1} \right) = n_p L_m \left(i_{d1} i_{q2} - i_{q1} i_{d2} \right) \quad (11)$$

4. Equation of motion

Т. 9. №6. 2023
https://doi.org/10.33619/2414-2948/91

$$T_L - T_e = \frac{J}{n_p}\frac{d\omega_r}{dt} \tag{12}$$

5. Power equation. The active power and reactive power of the stator are respectively:

$$\begin{cases} P_1 = u_{d1}i_{d1} + u_{q1}i_{q1} \\ Q_1 = u_{d1}i_{q1} + u_{q1}i_{d1} \end{cases} \tag{13}$$

The active power and reactive power of the rotor are respectively:

$$\begin{cases} P_2 = u_{d2}i_{d2} + u_{q2}i_{q2} \\ Q_2 = u_{d2}i_{q2} + u_{q2}i_{d2} \end{cases} \tag{14}$$

The above is the mathematical model of all doubly fed induction generators in synchronous coordinate system. Using these models, we can establish the state equation of induction generator for simulation [11].

Simulation model of doubly fed induction motor. In order to facilitate the later modeling and simulation and reduce the workload of building the motor model in the simulation, this paper adopts the "Asynchronous Machine SI Units" provided by Matlab/Simulink [12].

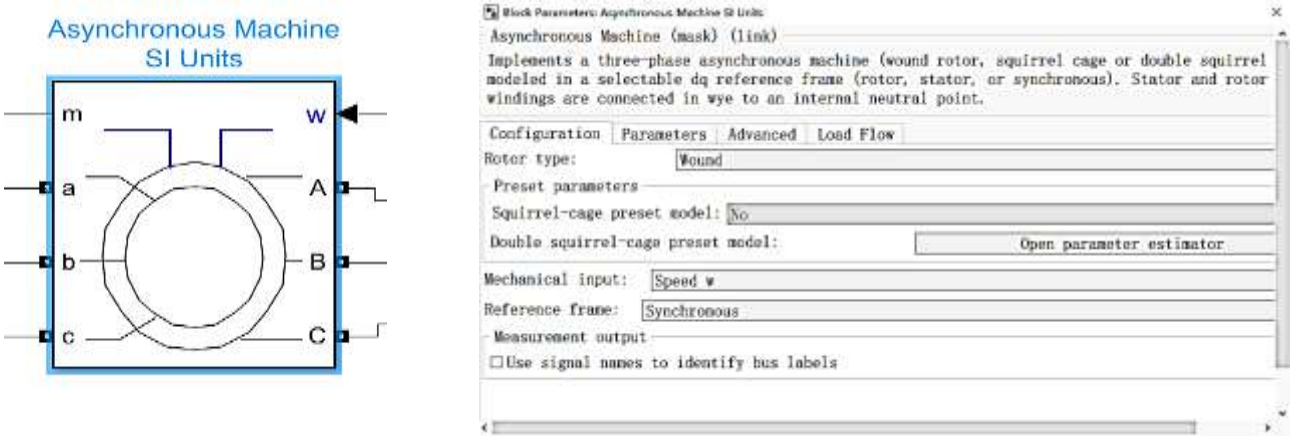

Figure 1. Simulink model of doubly fed induction motor

Mathematical model of voltage source dual PWM converter. The structure of Dual PWM voltage source converter is shown in

Figure **2.**.

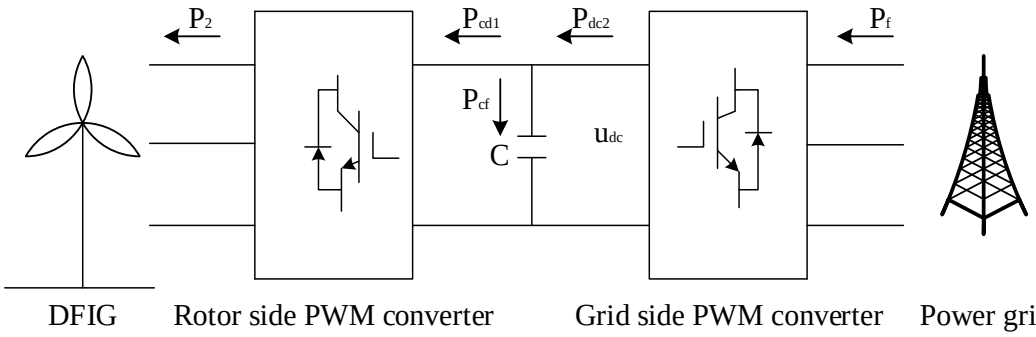

Figure 2. Back to back Dual PWM voltage source converter topology

Т. 9. №6. 2023
https://doi.org/10.33619/2414-2948/91

In the figure, P_2 is the active power absorbed by the rotor side of doubly fed machine. P_f is the active power absorbed by the back-to-back PWM converter from the power grid.P_{cf} represents the active power of the current flowing in the capacitor, which is stored in the capacitor without considering the capacitor loss. P_{dc1} is the DC input power of the rotor side converter. P_{dc2} is the DC output power of the grid side converter, which is the load power. u_{dc} is the DC bus voltage [13–15].

Modeling of grid side converter. The three-phase structure of the grid side PWM converter adopts the three-phase half bridge structure. The voltage is supplied to the converter through the transformer and connected to the AC side of the three-phase bridge after inductive filtering. The part of the bridge arm is composed of power switch tubes and parallel diodes, and the large capacitance is connected to the DC side. Suppose the model is an ideal model [13]:

1. The voltage connected to the power frequency power grid is an ideal three-phase sine wave.
2. Ideal linear unsaturated inductance is adopted.
3. Ideal diode and switch tube are adopted.

The corresponding main circuit topology can be obtained, as shown in Figure 3.

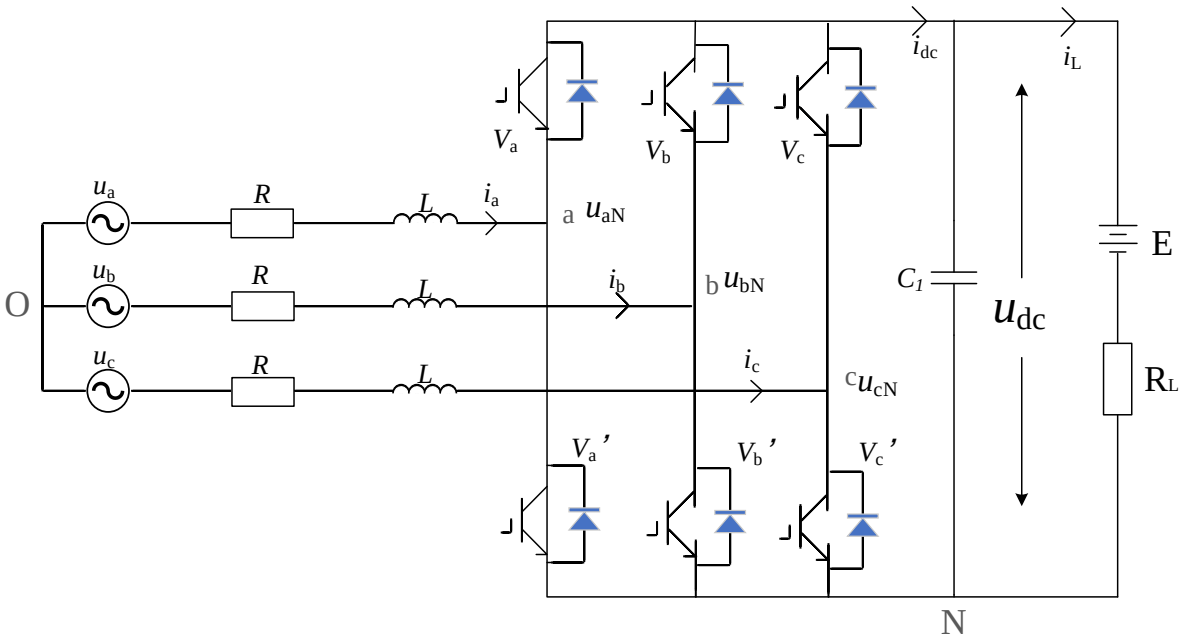

Figure 3. Main circuit topology of grid side PWM converter

In Figure 3, C_1 is the filter capacitor. u_k and i_k are the voltage and current of AC side respectively. Capacitance L and resistance R are the incoming inductance and its equivalent resistance respectively. According to Kirchhoff voltage law, the mathematical model of grid side converter is:

$$u_a = Ri_a + L\frac{di_a}{dt} + u_{aN} + u_{NO}, \quad (15)$$

$$u_b = Ri_b + L\frac{di_b}{dt} + u_{bN} + u_{NO} \quad (16)$$

$$u_c = Ri_c + L\frac{di_c}{dt} + u_{cN} + u_{NO}, \quad (17)$$

$$C\frac{du_{dc}}{dt} = i_{dc} - i_L \quad (18)$$

Т. 9. №6. 2023
https://doi.org/10.33619/2414-2948/91

Where, u_a,u_b,$u_c$are the phase voltage at the grid side. i_a,i_b,$i_c$are the phase currents at the grid side. i_L is the load current at DC side. u_{dc} is DC bus voltage. L and R are equivalent inductance and resistance at AC side [14].

In this paper, the power switch is equivalent to the unipolar binary logic switching function. The unipolar binary logic switching function is defined as follows:

$$S_k = \begin{cases} 1, The\ upper\ bridge\ arm\ is\ on\ a \quad the\ lower\ bridge\ arm\ is\ off \\ 0, The\ upper\ bridge\ arm\ is\ off\ and\ the\ lower\ bridge\ arm\ is\ on \end{cases} \quad (19)$$

Therefore, the bridge arm voltage of the converter can be expressed as:

$$u_{kN} = S_k u_{dc}\ (k = a, b, c), \quad (20)$$

According to the assumption, the power supply is an ideal power supply, that is, the three-phase power grid is balanced, and the sum of currents is 0, which can be obtained from equations (14-15):

$$u_{NO} = -\frac{u_{dc}}{3}(S_a + S_b + S_c) \quad (21)$$

Combined formula (18) (19) (20) can simplify formula (14) (15) (16) to:

$$l\frac{di_a}{dt} + Ri_a = u_a - (S_a - \frac{S_a+S_b+S_c}{3})u_{dc}, \quad (22)$$

$$l\frac{di_b}{dt} + Ri_b = u_b - (S_b - \frac{S_a+S_b+S_c}{3})u_{dc}, \quad (23)$$

$$l\frac{di_c}{dt} + Ri_c = u_c - (S_c - \frac{S_a+S_b+S_c}{3})u_{dc},, \quad (24)$$

Equation (21), (22), (23) is the mathematical model of grid side converter in three-phase static coordinate system. This section may be divided by subheadings. It should provide a concise and precise description of the experimental results, their interpretation, as well as the experimental conclusions that can be drawn. R_L is the equivalent load on the DC side. The design of the control system is simplified, and the time variable in the three-phase static coordinate system is transformed into the direct current in the d-q coordinate system.

The transformation matrix used for coordinate transformation is [16–17]:

$$T_{3s/2r} = \sqrt{\frac{2}{3}}\begin{bmatrix} cos\theta & cos(\theta - 120^\circ) & cos(\theta + 120^\circ) \\ -sin\theta & -sin(\theta - 120^\circ) & -sin(\theta + 120^\circ) \end{bmatrix}, \quad (25)$$

Thus, the mathematical model of grid side converter in rotating d-q coordinate system can be obtained:

$$l\frac{di_{ds}}{dt} = u_d - S_d u_{dc} + wli_{qs} - Ri_{ds}, \quad (26)$$

$$l\frac{di_{qs}}{dt} = u_q - S_q u_{dc} - wli_{ds} - Ri_{qs}, \quad (27)$$

$$C\frac{du_{dc}}{dt} = (i_{ds}S_d + i_{qs}S_q - i_L), \quad (28)$$

Grid voltage oriented vector control of grid side converter. It can be seen from the above section that in addition to the influence of i_{ds} and i_{qs}, the current cross coupling terms wli_{ds} and

Т. 9. №6. 2023
https://doi.org/10.33619/2414-2948/91

wli_{qs} , grid voltage u_d and u_q also affect the DQ axis current.Therefore, this paper adopts the grid voltage oriented vector control strategy to eliminate the current coupling and grid voltage disturbance. Grid voltage orientation is a control strategy that orients the d-axis of synchronous rotating dq coordinate system to the direction of grid voltage vector. The control method is simple, the switching frequency is stable, and the advanced SVPWM vector modulation technology is adopted [18]. The DQ component after grid voltage orientation is:

$$\begin{cases} u_d = u_s \\ u_q = 0 \end{cases} \tag{29}$$

Send:

$$\begin{cases} u'_{ds} = \frac{di_{ds}}{dt} + Ri_{ds} \\ u'_{qs} = \frac{di_{qs}}{dt} + Ri_{qs} \end{cases}, \begin{cases} \Delta u_{ds} = w_1 li_{qs} \\ \Delta u_{qs} = w_1 li_{ds} \end{cases} \tag{30}$$

Then equation (21) (22) (23) can be rewritten as:

$$\begin{cases} u_{ds} = -u'_{ds} + \Delta u_{ds} + u_d \\ u_{qs} = -u'_{qs} + \Delta u_{qs} + u_q \end{cases}, \tag{31}$$

Substitute equation (24) into equation (27):

$$\begin{cases} u_{ds} = -u'_{ds} + \Delta u_{ds} + u_s \\ u_{qs} = -u'_{qs} - \Delta u_{qs} \end{cases}, \tag{32}$$

In the above formula, u'_{ds} and u'_{qs} are the decoupling terms with first-order differential relationship with i_{ds} and i_{qs} respectively. $\Delta u_{ds}$and $\Delta u_{qs}$are the compensation terms to eliminate the cross coupling term, plus the introduction of voltage light gray compensation, so that the DQ axis current can realize independent decoupling control. According to the instantaneous power relationship:

$$\begin{cases} P = (u_d i_{ds} + u_q i_{qs}) = u_s i_{ds} \\ Q = (u_q i_{ds} + u_d i_{qs}) = -u_s i_{qs} \end{cases}, \tag{33}$$

From the above analysis, it can be concluded that adjusting i_{ds} and i_{qs} can control the grid side converter to absorb (or feed out) active power and reactive power, and realize the decoupling control of converters P and Q [19]. The simulation model of the system is built in Matlab / Simulink simulation software, as shown in Figure 4.

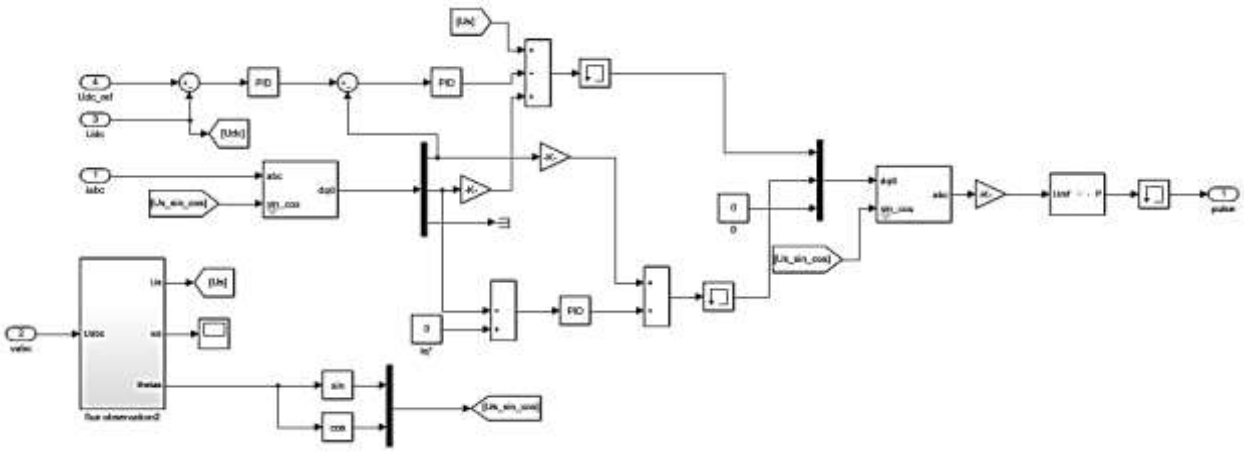

Figure 4. Simulation model of grid side PWM converter control

Т. 9. №6. 2023
https://doi.org/10.33619/2414-2948/91

The amplitude calculation method of AC voltage shown in Figure 6 first converts the grid side voltage u_{abc} into the voltage in two-phase static coordinates, and then calculates the amplitude. In order to obtain the electrical angle of the power grid, the phase-locked loop PLL module of MATLAB is adopted [20].

Figure 5 shows the calculation method of transforming DQ variable into three-phase AC signal in rotating coordinates [16–17].

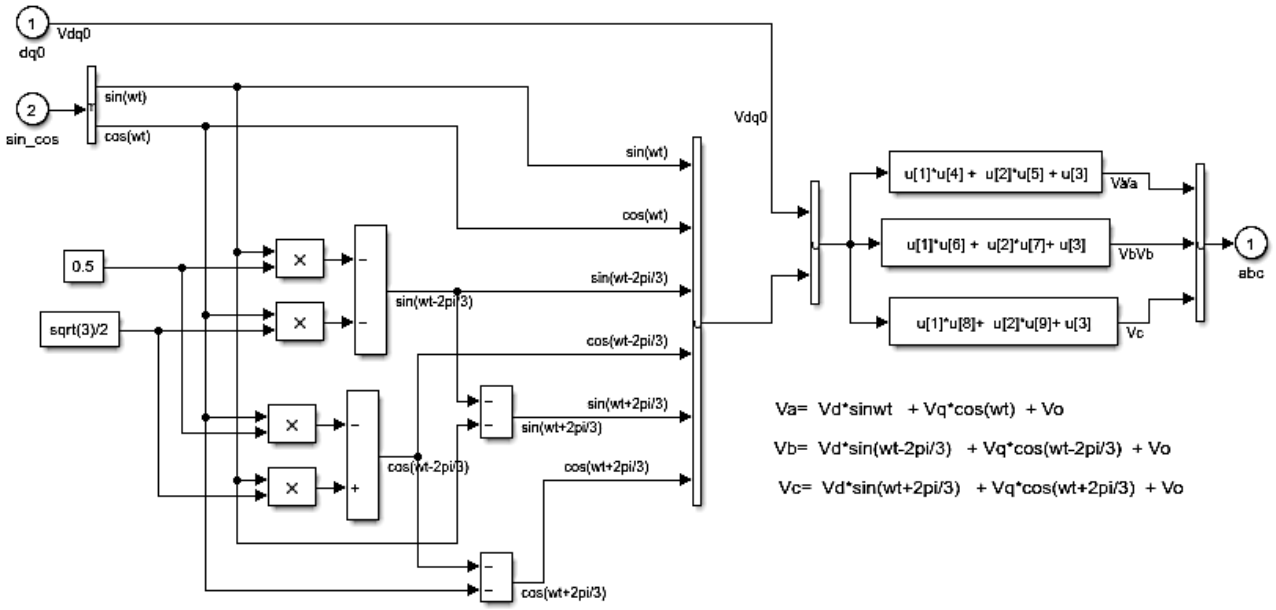

Figure 5. Calculation and simulation model of transforming DQ variable into three-phase AC signal in rotating coordinates

Simulation model of rotor side converter based on stator flux oriented vector control. During grid connected operation, the generator always operates at power frequency 50Hz. Under this frequency, the resistance of stator winding can be ignored, and the phase difference between stator flux vector and stator voltage vector of the generator is 90 degrees. In order to simplify the control of the system, the stator voltage vector or the total flux linkage of the stator winding is usually selected as the reference vector. In this section, the stator flux orientation is used to design the closed-loop control of doubly fed wind turbine [21].

Through the established mathematical model of doubly fed induction generator, the stator flux oriented vector control is adopted to make the d coordinate axis and stator flux Ψ_1 phase coincides to realize the decoupling of d-axis and q-axis variables:

$$\begin{cases} \Psi_{q1} = \Psi_1 \\ \Psi_{q1} = 0 \end{cases} \quad (34)$$

The stator winding is directly connected to the power grid. Due to the high voltage of the power grid, the voltage drop of the stator winding resistance can be ignored, so it is concluded that:

$$u_1 = e_1 = -\frac{d\Psi_1}{dt} \quad (35)$$

The phase voltage vector lags 90° behind the flux linkage vector. Since the stator is directly connected to the power grid and adopts the mode invariant matrix, in the two-phase coordinate system, the mode of the phase voltage comprehensive vector is the same as the phase voltage amplitude in the three-phase system, so:

Т. 9. №6. 2023
https://doi.org/10.33619/2414-2948/91

$$\begin{cases} u_{d1} = 0 \\ u_{q1} = -U_m \end{cases} \quad (36)$$

Where U_m is the phase voltage amplitude of three-phase system.

Therefore, it is concluded that:

$$\begin{cases} p\Psi_1 = 0 \\ \Psi_1 = U_m / w_1 \end{cases} \quad (37)$$

Then the equation of rotor excitation current is deduced as follows:

$$\begin{cases} i_{d2} = (-\Psi_1 + L_1 i_{d1})/L_m \\ i_{q2} = L_1 i_{d1}/L_m \end{cases} \quad (38)$$

Rotor flux linkage equation:

$$\begin{cases} \Psi_{d2} = -\dfrac{L_m}{L_1}\Psi_1 + L_2(1 - \dfrac{L_m^2}{L_1 L_2})i_{d2} = -a\Psi_1 + bi_{d2} \\ \Psi_{q2} = L_2(1 - \dfrac{L_m^2}{L_1 L_2})i_{q2} = bi_{q2} \end{cases} \quad (39)$$

Replace equation (35) into the voltage equation of rotor winding to obtain:

$$\begin{cases} u_{d2} = (R_2 + bp)i_{d2} - bw_1 i_{q2} = u'_{d2} + \Delta u_{d2} \\ u_{q2} = (R_2 + bp)i_{q2} - aw_1 \Psi_1 = u'_{q2} + \Delta u_{q2} \end{cases} \quad (40)$$

The decoupling control term u'_{d2} and u'_{q2} of rotor voltage is realized; Δu_{d2}, Δu_{q2} to offset the compensation term of cross coupling, the rotor voltage is decomposed into decoupling term and compensation term, which not only simplifies the control, but also ensures the accuracy of control and the rapidity of dynamic response [22-24]. The Simulink simulation model of stator flux vector control is shown in

There are mainly two sub modules in the model: d-axis reference voltage module and q-axis reference voltage module (Figure 6).

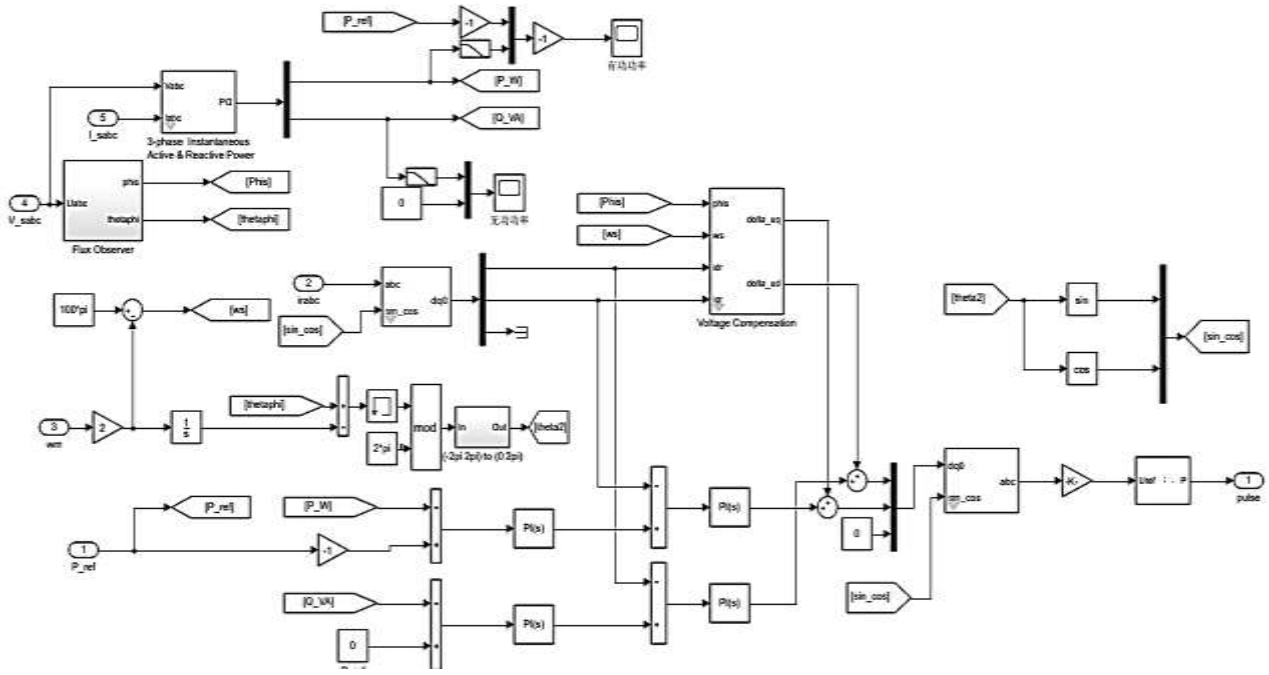

Figure 6. Vector control simulation model

Grid connection simulation model of variable speed constant frequency doubly fed induction wind power generation system. The simulation model of doubly fed induction wind turbine connected to grid operation is shown in the figure below. According to the optimal relationship curve

Т. 9. №6. 2023
https://doi.org/10.33619/2414-2948/91

between wind turbine speed and power, the reference output power can be derived from the relationship curve under the condition of changing wind speed. The reference output active power signal and the feedback signal of wind turbine output electric power are combined into a closed-loop control system, and then different power generation conditions are analyzed to select different corresponding reactive power reference values [25].

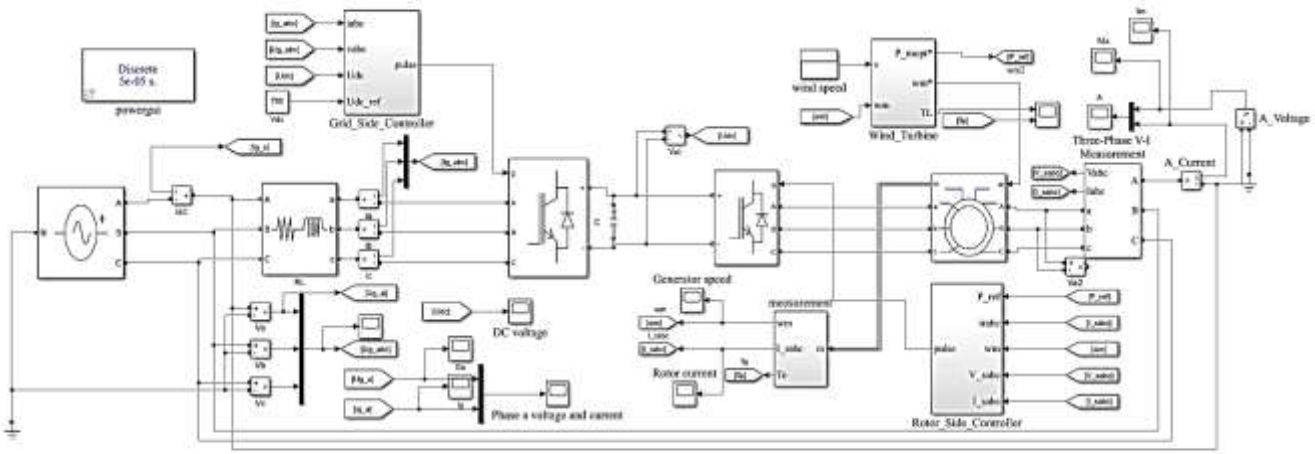

Figure 7. Variable speed constant frequency doubly fed induction wind power generation system

Results and discussion

In order to verify the feasibility and effectiveness of the control algorithm designed in this paper, the simulation model and retrograde simulation built in the previous section are studied.

Table

MAIN PARAMETER SETTING OF DOUBLY FED WIND TURBINE SYSTEM

Doubly fed generator	Power: P_n=25kW, Rated voltage U_n = 380V, Rated frequency f_n = 50Hz,The polar logarithm is 2, Stator resistance R_s = 0.435Ω, Stator leakage inductance 2mH, Rotor leakage inductance 3mH, Mutual inductance L_m = 69.31mH.
Wind turbine	The radius of the wind turbine is R = 4m, and the optimal tip speed ratio is 7.8.
Grid side PWM converter	Inductance 6mH, equivalent resistance 0.05Ω, support capacitance C = 2200μF.
Grid voltage and parameter setting	The rated power grid voltage is 380V, the frequency is 50Hz, the DC voltage reference value is set to 750V, and the PWM switching frequency is 10kHz.

In order to verify the dynamic performance of the system, the initial value of wind speed in the simulation is set as 6m/s, t = 1.5s, 10m/s and T = 2.5s, 12m/s. The simulation time is set to 4s.

Figure 8a shows the simulation results of DC bus voltage. It can be seen from Figure 13 that the actual value of DC voltage can quickly reach the reference value of 750V. Although there are some overshoot, about 8%, the time to reach the steady state for the first time is about 0.25s. When the wind speed of t = 1.5s and t = 2.5s suddenly changes, the DC voltage has a short decline process and soon returns to the reference value, which shows that the control algorithm has good control performance and dynamic performance [26].

Figure 8b shows the simulation results of phase A voltage and phase a current on the grid side. It can be seen from the figure that when the wind speed changes suddenly, the current also increases due to the increase of generator output power. In addition, in the whole change process, the phase of

Т. 9. №6. 2023
https://doi.org/10.33619/2414-2948/91

phase a voltage and phase a current always remain in phase, which shows that the unit power factor operation is realized. Figure 8c shows the simulation results of the mechanical angular velocity of the doubly fed generator. It can be seen from the figure that when the wind speed suddenly increases, the mechanical angular velocity of the generator will also increase. Figure 8d shows the simulation results of the three-phase current of the rotor on the machine side of the doubly fed generator. It can be seen from the figure that when the wind speed suddenly increases, the mechanical angular speed of the generator will also increase, and the power generated at this time will also increase, so that the current will gradually increase.

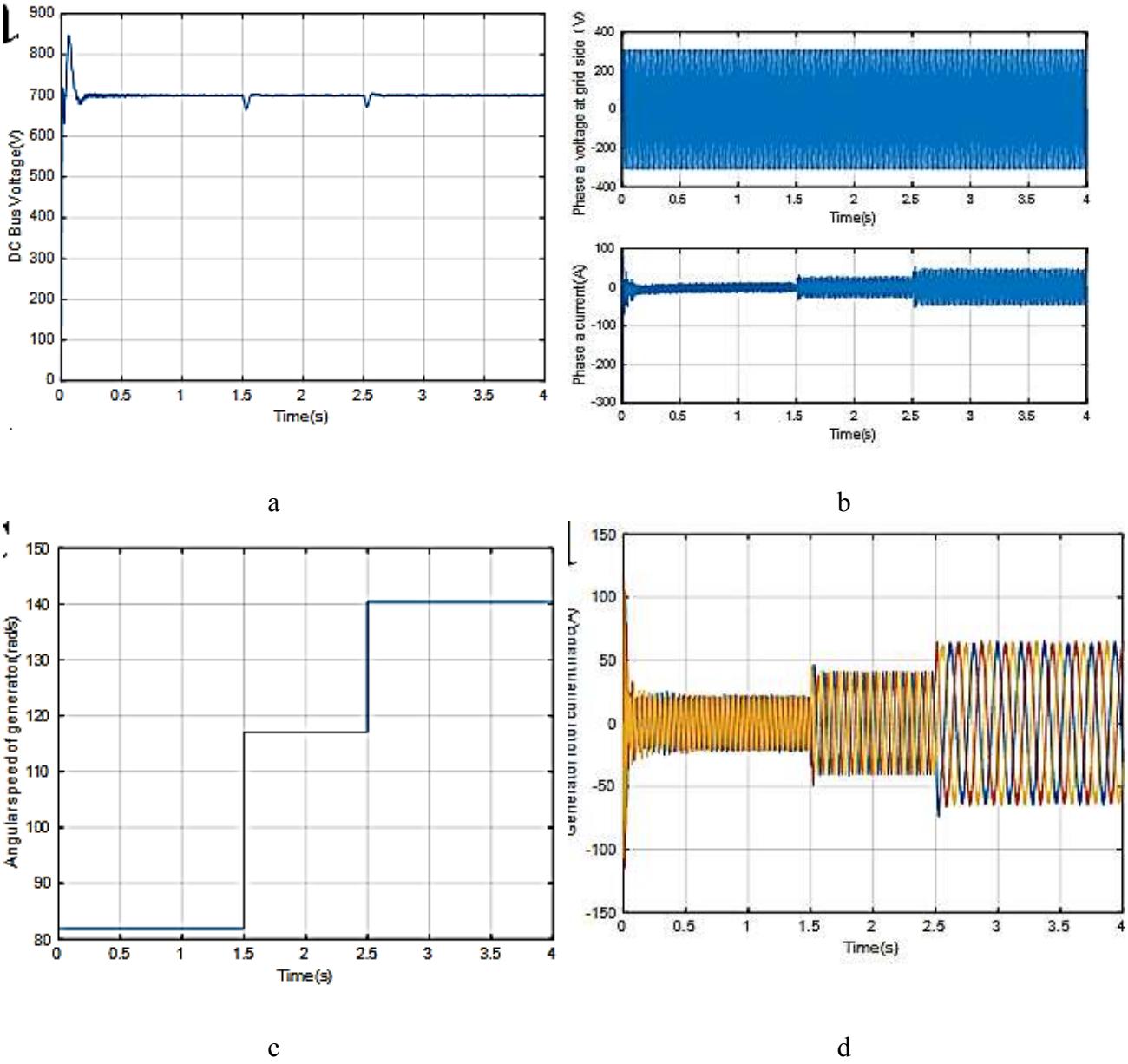

a b c d

Figure 8. Simulation results of DC bus voltage(a), phase A voltage and current on grid side(b), mechanical angular velocity of doubly fed generator(c) and rotor current of doubly fed generator(d)

Figure 9b and Figure 9c show the simulation results of the reference value and actual value of the active and reactive power of the power loop in the machine side control system of the doubly fed generator. It can be seen from the figure that when the wind speed increases abruptly, the mechanical angular speed of the generator will also increase, at this time, the issued active power will also

Т. 9. №6. 2023
https://doi.org/10.33619/2414-2948/91

increase, and the actual value can quickly track the reference value. It shows that the generator control system has good control performance. In addition, due to the increase of active power, the current will also increase, as shown in Figure 9a.

As a clean and renewable resource, wind energy will play an important role in the future energy field. With the continuous investment in wind power generation all over the world, VSCF wind power generation will develop continuously and stably. Although we are constantly exploring new VSCF schemes, doubly fed wind power generation system still occupies a high market share so far. In the future, it will still be one of the research hotspots in various countries.

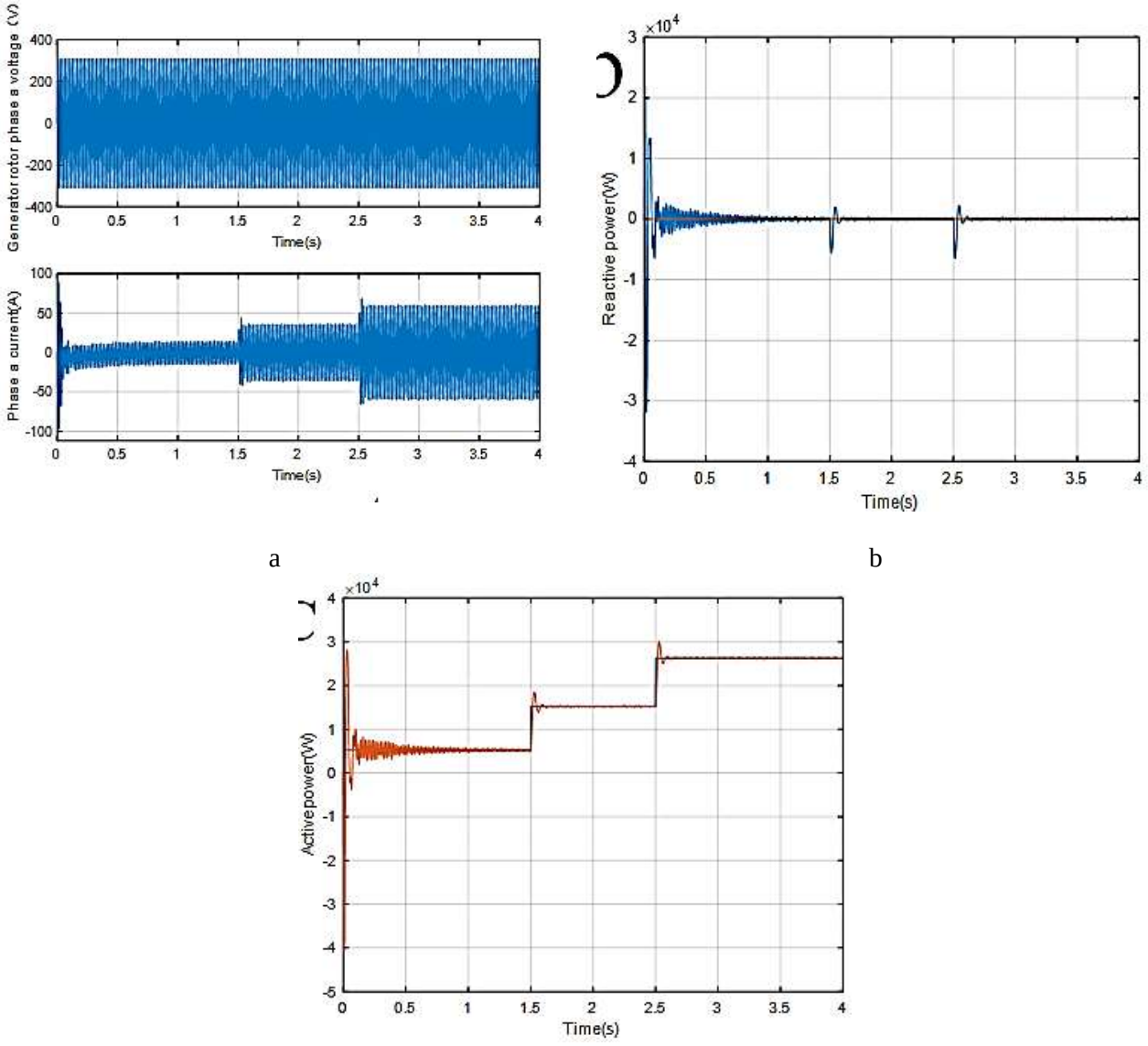

a b

c

Figure 9. Simulation of phase A voltage and phase A current on stator side of generator (a), reactive power reference value and actual value of doubly fed generator (b) and active power reference value and actual value of doubly fed generator (c)

This paper analyzes the basic operation principle of doubly fed generator, and establishes the mathematical models of doubly fed generator in three-phase static coordinate system and synchronous rotating coordinate system by using the principle of coordinate transformation. The double converter is used as the AC excitation power supply of doubly fed wind power generation

Т. 9. №6. 2023
https://doi.org/10.33619/2414-2948/91

system. The grid side converter and rotor side converter are discussed respectively, and the mathematical models are established respectively. Among them, the grid side converter adopts the grid voltage oriented vector control strategy and space vector pulse width modulation technology. The stator field oriented vector control strategy is adopted on the rotor side.

Through the simulation of the model established in this paper, the initial overshoot of DC bus voltage is about 8%, but this model has good dynamic performance. After 0.25s, the DC bus voltage can reach the steady state, and the actual value of DC bus voltage can soon reach the reference value of 750V. When the wind speed of t = 1.5s and t = 2.5s suddenly changes, the DC voltage has a short decline process and soon returns to the reference value, which shows that the model has good control performance and dynamic performance.

When the wind speed changes suddenly, the current also increases due to the increase of generator output power. In addition, in the whole change process, the phase of phase a voltage and phase a current always remain in phase, which shows that the model can well realize the operation of unity power factor. When the wind speed suddenly increases, the mechanical angular speed of the generator will also increase, and the active power will also increase, and the actual value can quickly track the reference value. Since the reference value of reactive power is set to 0, the actual reactive power can quickly track the reference value under the action of reactive power loop PI controller, which shows that the generator control system has good control performance.

Integrate the simulation models of each part to complete the construction of the simulation platform of the whole wind power generation system. The simulation results show that the mathematical model of each part is correct. The wind power generation system can decouple P and Q without affecting the amplitude and frequency of stator voltage under the change of wind speed.

References:

1. Mohd Zin, A. A. B., Pesaran HA, M., Khairuddin, A. B., Jahanshaloo, L., & Shariati, O. (2013). An overview on doubly fed induction generators′ controls and contributions to wind based electricity generation. *Renewable and Sustainable Energy Reviews*, *27*(C), 692-708. https://doi.org/10.1016/j.rser.2013.07.010

2. Rahimi, M. (2014). Dynamic performance assessment of DFIG-based wind turbines: A review. *Renewable and Sustainable Energy Reviews*, *37*, 852-866. https://doi.org/10.1016/j.rser.2014.05.072

3. Cheng, M., & Zhu, Y. (2014). The state of the art of wind energy conversion systems and technologies: A review. *Energy conversion and management*, *88*, 332-347. https://doi.org/10.1016/j.enconman.2014.08.037

4. Torkaman, H., & Keyhani, A. (2018). A review of design consideration for Doubly Fed Induction Generator based wind energy system. *Electric Power Systems Research*, *160*, 128-141. https://doi.org/10.1016/j.epsr.2018.02.012

5. Junyent-Ferré, A., Gomis-Bellmunt, O., Sumper, A., Sala, M., & Mata, M. (2010). Modeling and control of the doubly fed induction generator wind turbine. *Simulation Modelling Practice and Theory*, *18*(9), 1365-1381. https://doi.org/10.1016/j.simpat.2010.05.018

6. Simonetti, D. S., Amorim, A. E., & Oliveira, F. D. (2018). Doubly fed induction generator in wind energy conversion systems. In *Advances in Renewable Energies and Power Technologies* (pp. 461-490). Elsevier. https://doi.org/10.1016/B978-0-12-812959-3.00015-0

7. Chatterjee, A., & Chatterjee, D. (2015). An improved excitation control technique of three-phase induction machine operating as dual winding generator for micro-wind domestic application. *Energy Conversion and Management*, *98*, 98-106. https://doi.org/10.1016/j.enconman.2015.03.091

8. Poitiers, F., Bouaouiche, T., & Machmoum, M. (2009). Advanced control of a doubly-fed induction generator for wind energy conversion. *Electric Power Systems Research*, *79*(7), 1085-1096. https://doi.org/10.1016/j.epsr.2009.01.007

9. Soares, O., Gonçalves, H., Martins, A., & Carvalho, A. (2010). Nonlinear control of the doubly-fed induction generator in wind power systems. *Renewable Energy*, *35*(8), 1662-1670. https://doi.org/10.1016/j.renene.2009.12.008

10. Jovanović, M., & Chaal, H. (2017). Wind power applications of doubly-fed reluctance generators with parameter-free hysteresis control. *Energy Conversion and Management*, *134*, 399-409. https://doi.org/10.1016/j.enconman.2016.10.064

11. Egea-Alvarez, A., Junyent-Ferre, A., Bergas-Jane, J., Bianchi, F. D., & Gomis-Bellmunt, O. (2014). Control of a wind turbine cluster based on squirrel cage induction generators connected to a single VSC power converter. *International Journal of Electrical Power & Energy Systems*, *61*, 523-530. https://doi.org/10.1016/j.ijepes.2014.03.069

12. Ghennam, T., & Berkouk, E. M. (2010). Back-to-back three-level converter controlled by a novel space-vector hysteresis current control for wind conversion systems. *Electric Power Systems Research*, *80*(4), 444-455. https://doi.org/10.1016/j.epsr.2009.10.009

13. Taveiros, F. E. V., Barros, L. S., & Costa, F. B. (2015). Back-to-back converter state-feedback control of DFIG (doubly-fed induction generator)-based wind turbines. *Energy*, *89*, 896-906. https://doi.org/10.1016/j.energy.2015.06.027

14. Chai, Z., Li, H., Xie, X., Abdeen, M., Yang, T., & Wang, K. (2021). Output impedance modeling and grid-connected stability study of virtual synchronous control-based doubly-fed induction generator wind turbines in weak grids. *International Journal of Electrical Power & Energy Systems*, *126*, 106601. https://doi.org/10.1016/j.ijepes.2020.106601

15. Bedoud, K., Rhif, A., Bahi, T., & Merabet, H. (2018). Study of a double fed induction generator using matrix converter: Case of wind energy conversion system. *International Journal of Hydrogen Energy*, *43*(25), 11432-11441. https://doi.org/10.1016/j.ijhydene.2017.07.010

16. Cárdenas, R., Pena, R., Wheeler, P., Clare, J., Munoz, A., & Sureda, A. (2013). Control of a wind generation system based on a Brushless Doubly-Fed Induction Generator fed by a matrix converter. *Electric Power Systems Research*, *103*, 49-60. https://doi.org/10.1016/j.epsr.2013.04.006

17. Hu, S., & Zhu, G. (2022). Enhanced control and operation for brushless doubly-fed induction generator based wind turbine system under grid voltage unbalance. *Electric Power Systems Research*, *207*, 107861. https://doi.org/10.1016/j.epsr.2022.107861

18. Akel, F., Ghennam, T., Berkouk, E. M., & Laour, M. (2014). An improved sensorless decoupled power control scheme of grid connected variable speed wind turbine generator. *Energy Conversion and Management*, *78*, 584-594. https://doi.org/10.1016/j.enconman.2013.11.015

19. Yousefi-Talouki, A., Pouresmaeil, E., & Jørgensen, B. N. (2014). Active and reactive power ripple minimization in direct power control of matrix converter-fed DFIG. *International Journal of Electrical Power & Energy Systems*, *63*, 600-608. https://doi.org/10.1016/j.ijepes.2014.06.041

20. Phan, D. C., & Yamamoto, S. (2016). Rotor speed control of doubly fed induction generator wind turbines using adaptive maximum power point tracking. *Energy*, *111*, 377-388. https://doi.org/10.1016/j.energy.2016.05.077

21. Gayen, P. K., Chatterjee, D., & Goswami, S. K. (2015). Stator side active and reactive power control with improved rotor position and speed estimator of a grid connected DFIG (doubly-fed induction generator). *Energy*, *89*, 461-472. https://doi.org/10.1016/j.energy.2015.05.111

22. Choi, S., Kang, Y. C., Kim, K. H., Lee, Y. I., & Terzija, V. (2021). A frequency-

responsive power-smoothing scheme of a doubly-fed induction generator for enhancing the energy-absorbing capability. *International Journal of Electrical Power & Energy Systems*, *131*, 107053. https://doi.org/10.1016/j.ijepes.2021.107053

23. Wiam, A., & Ali, H. (2019). Direct torque control-based power factor control of a DFIG. *Energy Procedia*, *162*, 296-305. https://doi.org/10.1016/j.egypro.2019.04.031

24. Kaloi, G. S., Wang, J., & Baloch, M. H. (2016). Active and reactive power control of the doubly fed induction generator based on wind energy conversion system. *Energy Reports*, *2*, 194-200. https://doi.org/10.1016/j.egyr.2016.08.001

25. da Silva, K. F., & Saidel, M. A. (2010). Digital control and integration of a 192 MW wind farm with doubly fed induction generator into the Brazilian power system. *Electric power systems research*, *80*(1), 108-114. https://doi.org/10.1016/j.epsr.2009.08.010

26. Luo, X. (2021). Design of an adaptive controller for double-fed induction wind turbine power. *Energy Reports*, *7*, 1622-1626. https://doi.org/10.1016/j.egyr.2021.09.047

Список литературы:

1. Mohd Zin A. A. B., Pesaran H. A., M., Khairuddin A. B., Jahanshaloo L., Shariati O. An overview on doubly fed induction generators′ controls and contributions to wind based electricity generation // Renewable and Sustainable Energy Reviews. 2013. V. 27. №C. P. 692-708. https://doi.org/10.1016/j.rser.2013.07.010

2. Rahimi M. Dynamic performance assessment of DFIG-based wind turbines: A review // Renewable and Sustainable Energy Reviews. 2014. V. 37. P. 852-866. https://doi.org/10.1016/j.rser.2014.05.072

3. Cheng M., Zhu Y. The state of the art of wind energy conversion systems and technologies: A review // Energy conversion and management. 2014. V. 88. P. 332-347. https://doi.org/10.1016/j.enconman.2014.08.037

4. Torkaman H., Keyhani A. A review of design consideration for Doubly Fed Induction Generator based wind energy system // Electric Power Systems Research. 2018. V. 160. P. 128-141. https://doi.org/10.1016/j.epsr.2018.02.012

5. Junyent-Ferré A., Gomis-Bellmunt O., Sumper A., Sala M., Mata M. Modeling and control of the doubly fed induction generator wind turbine // Simulation Modelling Practice and Theory. 2010. V. 18. №9. P. 1365-1381. https://doi.org/10.1016/j.simpat.2010.05.018

6. Simonetti D. S. L., Amorim A. E. A., Oliveira F. D. C. Doubly fed induction generator in wind energy conversion systems // Advances in Renewable Energies and Power Technologies. Elsevier, 2018. P. 461-490. https://doi.org/10.1016/B978-0-12-812959-3.00015-0

7. Chatterjee A., Chatterjee D. An improved excitation control technique of three-phase induction machine operating as dual winding generator for micro-wind domestic application // Energy Conversion and Management. 2015. V. 98. P. 98-106. https://doi.org/10.1016/j.enconman.2015.03.091

8. Poitiers F., Bouaouiche T., Machmoum M. Advanced control of a doubly-fed induction generator for wind energy conversion // Electric Power Systems Research. 2009. V. 79. №7. P. 1085-1096. https://doi.org/10.1016/j.epsr.2009.01.007

9. Soares O., Gonçalves H., Martins A., Carvalho A. Nonlinear control of the doubly-fed induction generator in wind power systems // Renewable Energy. 2010. V. 35. №8. P. 1662-1670. https://doi.org/10.1016/j.renene.2009.12.008

10. Jovanović M., Chaal H. Wind power applications of doubly-fed reluctance generators with parameter-free hysteresis control // Energy Conversion and Management. 2017. V. 134. P. 399-409.

https://doi.org/10.1016/j.enconman.2016.10.064

11. Egea-Alvarez, A., Junyent-Ferre, A., Bergas-Jane, J., Bianchi, F. D., & Gomis-Bellmunt, O. Control of a wind turbine cluster based on squirrel cage induction generators connected to a single VSC power converter // International Journal of Electrical Power & Energy Systems. 2014. V. 61. P. 523-530. https://doi.org/10.1016/j.ijepes.2014.03.069

12. Ghennam T., Berkouk E. M. Back-to-back three-level converter controlled by a novel space-vector hysteresis current control for wind conversion systems // Electric Power Systems Research. 2010. V. 80. №4. P. 444-455. https://doi.org/10.1016/j.epsr.2009.10.009

13. Taveiros F. E. V., Barros L. S., Costa F. B. Back-to-back converter state-feedback control of DFIG (doubly-fed induction generator)-based wind turbines // Energy. 2015. V. 89. P. 896-906. https://doi.org/10.1016/j.energy.2015.06.027

14. Chai Z., Li H., Xie X., Abdeen M., Yang T., Wang K. Output impedance modeling and grid-connected stability study of virtual synchronous control-based doubly-fed induction generator wind turbines in weak grids // International Journal of Electrical Power & Energy Systems. 2021. V. 126. P. 106601. https://doi.org/10.1016/j.ijepes.2020.106601

15. Bedoud K., Rhif A., Bahi T., Merabet H. Study of a double fed induction generator using matrix converter: Case of wind energy conversion system // International Journal of Hydrogen Energy. 2018. V. 43. №25. P. 11432-11441. https://doi.org/10.1016/j.ijhydene.2017.07.010

16. Cárdenas R., Pena R., Wheeler P., Clare J., Munoz A., Sureda A. Control of a wind generation system based on a Brushless Doubly-Fed Induction Generator fed by a matrix converter // Electric Power Systems Research. 2013. V. 103. P. 49-60. https://doi.org/10.1016/j.epsr.2013.04.006

17. Hu S., Zhu G. Enhanced control and operation for brushless doubly-fed induction generator based wind turbine system under grid voltage unbalance // Electric Power Systems Research. 2022. V. 207. P. 107861. https://doi.org/10.1016/j.epsr.2022.107861

18. Akel F., Ghennam T., Berkouk E. M., Laour M. An improved sensorless decoupled power control scheme of grid connected variable speed wind turbine generator // Energy Conversion and Management. 2014. V. 78. P. 584-594. https://doi.org/10.1016/j.enconman.2013.11.015

19. Yousefi-Talouki A., Pouresmaeil E., Jørgensen B. N. Active and reactive power ripple minimization in direct power control of matrix converter-fed DFIG // International Journal of Electrical Power & Energy Systems. 2014. V. 63. P. 600-608. https://doi.org/10.1016/j.ijepes.2014.06.041

20. Phan D. C., Yamamoto S. Rotor speed control of doubly fed induction generator wind turbines using adaptive maximum power point tracking // Energy. 2016. V. 111. P. 377-388. https://doi.org/10.1016/j.energy.2016.05.077

21. Gayen P. K., Chatterjee D., Goswami S. K. Stator side active and reactive power control with improved rotor position and speed estimator of a grid connected DFIG (doubly-fed induction generator) // Energy. 2015. V. 89. P. 461-472. https://doi.org/10.1016/j.energy.2015.05.111

22. Choi S., Kang Y. C., Kim K. H., Lee Y. I., Terzija V. A frequency-responsive power-smoothing scheme of a doubly-fed induction generator for enhancing the energy-absorbing capability // International Journal of Electrical Power & Energy Systems. 2021. V. 131. P. 107053. https://doi.org/10.1016/j.ijepes.2021.107053

23. Wiam A., Ali H. Direct torque control-based power factor control of a DFIG // Energy Procedia. 2019. V. 162. P. 296-305. https://doi.org/10.1016/j.egypro.2019.04.031

24. Kaloi G. S., Wang J., Baloch M. H. Active and reactive power control of the doubly fed induction generator based on wind energy conversion system // Energy Reports. 2016. V. 2. P. 194-200. https://doi.org/10.1016/j.egyr.2016.08.001

25. Da Silva K. F., Saidel M. A. Digital control and integration of a 192 MW wind farm with doubly fed induction generator into the Brazilian power system // Electric power systems research. 2010. V. 80. №1. P. 108-114. https://doi.org/10.1016/j.epsr.2009.08.010

26. Luo X. Design of an adaptive controller for double-fed induction wind turbine power // Energy Reports. 2021. V. 7. P. 1622-1626. https://doi.org/10.1016/j.egyr.2021.09.047

Работа поступила
в редакцию 08.05.2023 г.

Принята к публикации
14.05.2023 г.

Ссылка для цитирования:

Zheng Shouqing, Bai Yike, Hou Ruida, Wang Bao Liang Research on Modeling and Simulation of Doubly Fed Induction Wind Turbine Based on Matlab/Simulink // Бюллетень науки и практики. 2023. Т. 9. №6. С. 309-326. https://doi.org/10.33619/2414-2948/91/39

Cite as (APA):

Zheng, Shouqing, Bai, Yike, Hou, Ruida, & Wang, Bao Liang (2023). Research on Modeling and Simulation of Doubly Fed Induction Wind Turbine Based on Matlab/Simulink. *Bulletin of Science and Practice, 9*(6), 309-326. https://doi.org/10.33619/2414-2948/91/39